Mode Selection and Shape Transitions of Phospholipid Monolayer Domains

T. K. Vanderlick and H. Möhwald*

Universität Mainz, Institut für Physikalische Chemie, D-6500 Mainz, West Germany
(Received: June 12, 1989)

Above a critical surface pressure, lipid monolayers at the air/water interface form gellike domains which coexist with a less dense fluid phase. In this work, we employ the free energy theory of McConnell and co-workers to predict the shapes and associated shape transitions of regularly undulating lipid domains, i.e., domains with boundaries that undulate with a characteristic mode and relative amplitude. The equilibrium shape is determined by a dimensionless number, Γ, which relates the importance of repulsive electrostatic interactions arising from the dipole moments of the lipid molecules to the effect of line tension. Shape transitions are predicted between successive modes as Γ is varied. While the mode of the shape with the lowest free energy increases with Γ, the relative amplitude of the undulation asymptotes to a limit. We also consider mixed-mode shapes formed by combining two distinct modes. For the cases examined, we find no evidence of mode coupling. We also show how the analysis can be used to interpret experimental observations, at fixed Γ, of the shapes of lipid domains as their area is varied. Shape transitions between higher order modes are predicted as the area is increased; over the range of areas where a given mode is the most stable, the relative amplitude of the undulation increases with increasing area.

Introduction

In addition to their biological significance,[1,2] phospholipid molecules are ideally suited for the study of self-assembly and associated phase transitions. It is now well established that certain lipid monolayers at the air/water interface undergo a first-order phase transition between a fluid and a more condensed gel phase.[3,4] In this two-phase regime, the gel phase exists as discrete domains within the continuous fluid phase. Using epifluorescence microscopy,[5-7] it is possible to visualize these gel domains and hence directly examine their growth, sizes, and shapes.

One of the most interesting features of this domain formation is the variety of shapes that can develop. Miller and Möhwald have, for example, observed fractal structures whose growth is governed by diffusion-limited aggregation.[8,9] Such domains, however, anneal after time into their equilibrium shapes. Apart from the fascinating nonequilibrium microstructures and shapes that can occur, domains in equilibrium with the surrounding fluid phase can also exhibit a host of shapes that depend not only on the particular lipid system but also on the thermodynamic-state variables. While regular disklike domains can often be observed,[10,11] many lipid systems form domains with shapes that are distinctly noncircular.

Lipid molecules at the air/water interface exhibit permanent dipole moments that are partially aligned to the surface. Those lipids with dissociable head groups can also possess a net surface charge. The more condensed gel phase therefore exhibits an excess dipole moment, and possibly an excess charge, relative to the fluid phase. Long-range electrostatic interactions between the lipid molecules control both the formation and shapes of the gel-phase domains[3] and in general play an important role in the phase behavior of these two-dimensional systems.

Andelman et al.[12,13] have examined the effect of long-range dipolar forces on the phase behavior of insoluble monolayers. Using a free energy analysis, they found that repulsive electrostatic interactions can stabilize inhomogeneous monolayers for which the in-plane concentration is undulating. They predicted the existence of, and associated phase transitions between, ordered microstructures composed of stripelike (smectic), hexagonal, and inverted hexagonal phases.

A similar free energy analysis was developed by McConnell and co-workers[14] to predict the equilibrium shapes of isolated finite lipid domains. Within a single domain, the effect of repulsive electrostatic interactions is to maximize the average distance between molecules, thus favoring elongated, noncompact shapes. Opposing this tendency is the effect of line tension between the gel domain and the surrounding fluid phase. The line tension acts to minimize the interfacial area, thus favoring compact shapes. Using their theory, McConnell and co-workers showed that under specified conditions isolated domains can exhibit shape transitions. In particular, they analytically determined the conditions for various shape transitions such as circular to elliptical domains[15] and square to rectangular domains.[16]

One class of shapes that has often been experimentally observed consists of shapes with nearly periodic undulating boundaries. One such example is shown in Figure 1, taken from the work of Flörsheimer.[17] Shown here is the growth of an isolated lipid L-α-dipalmitoylphosphatidylcholine (DPPC) domain held in a fixed position by using an electrode mounted above the water surface.[18-20] The observation of such shapes has motivated us to examine the shape transitions of dipolar lipid domains between regularly undulating shapes characterized by discrete modes, for which the circular shape is a special (zeroth mode) case.

Governing Equations

Following the theory of McConnell and co-workers,[14-16] the total free energy of an isolated dipolar domain can be expressed as

(1) Phillips, M. C.; Chapman, D. *Biochim. Biophys. Acta* **1968**, *163*, 301.
(2) Verger, R.; Pattus, F.; Pieroni, G.; Riviere, C.; Ferrato, F.; Leonardi, J.; Dargent, B. *Colloid Surf.* **1984**, *10*, 163.
(3) Fischer, A.; Lösche, M.; Möhwald, H.; Sackmann, E. *J. Phys. Lett.* **1984**, *5*, L785-L791.
(4) McConnell, H. M.; Tamm, L.; Weiss, R. M. *Proc. Natl. Acad. Sci. U.S.A.* **1984**, *81*, 3249-3253.
(5) Lösche, M.; Sackmann, E.; Möhwald, H. *Ber. Bunsen-Ges. Phys. Chem.* **1983**, *87*, 848-852.
(6) Peters, R.; Beck, K. *Proc. Natl. Acad. Sci. U.S.A.* **1983**, *80*, 7183-7187.
(7) Weiss, R. M.; McConnell, H. M. *Nature* **1984**, *310*, 47-49.
(8) Miller, A.; Möhwald, H. *J. Chem. Phys.* **1987**, *86*, 4258-4265.
(9) Miller, A.; Knoll, W.; Möhwald, H. *Phys. Rev. Lett.* **1986**, *56*, 2633-2636.
(10) Helm, C. A.; Möhwald, H. *J. Phys. Chem.* **1988**, *92*, 1262-1266.
(11) Lösche, M.; Duwe, H.-P.; Möhwald, H. *J. Colloid Interface Sci.* **1988**, *126*, 432-444.
(12) Keller, D. J.; McConnell, H. M.; Moy, V. T. *J. Phys. Chem.* **1986**, *90*, 2311-2315.
(13) Andelman, D.; Brochard, F.; de Gennes, P. G.; Joanny, J. F. *C. R. Seances Acad. Sci., Ser. C* **1985**, *301*, 675-678.
(14) Andelman, D.; Brochard, F.; Joanny, J. F. *J. Chem. Phys.* **1987**, *86*, 3673-3681.
(15) Keller, D. J.; Korb, J. P.; McConnell, H. M. *J. Phys. Chem.* **1987**, *91*, 6417-6422.
(16) McConnell, H. M.; Moy, V. T. *J. Phys. Chem.* **1988**, *92*, 4520-4525.
(17) Flörsheimer, M. Thesis, TU Munich, 1989.
(18) Miller, A.; Möhwald, H. *Europhys. Lett.* **1986**, *2*, 67-74.
(19) Heckl, W. M.; Miller, A.; Möhwald, H. *Thin Solid Films* **1988**, *159*, 125-132.
(20) Flörsheimer, M.; Möhwald, H. *Chem. Phys. Lipids* **1989**, *49*, 231-241.

0022-3654/90/2094-0886$02.50/0

$$F = F^{I} + F^{E} + F^{\dagger} \tag{1}$$

where F^{I} represents the interfacial contribution to the free energy, F^{E} represents the electrostatic energy associated with the dipoles which constitute the domain, and $F^{\dagger}$ accounts for any remaining, shape-independent, contributions to the total free energy.

Assuming that the interface can be approximated as a discontinuity between the two phases, characterized by a line tension λ, F^{I} is given by

$$F^{I} = \lambda P \tag{2}$$

where P is the perimeter of the domain. The electrostatic energy of the dipolar domain is given by

$$F^{E} = \frac{1}{2}\mu^2 \int\int \left[\frac{1}{|\mathbf{r} - \mathbf{r}'|^3} + \frac{4\pi}{3}\delta^3(\mathbf{r}) \right] dA\, dA' \tag{3}$$

where μ is the excess dipole density, i.e., the difference in dipole moment per unit area between the gel and fluid phases, and δ is the Dirac delta function. Because the integrand diverges as the distance between dipoles goes to zero, the integrand must be constrained to values such that $|\mathbf{r} - \mathbf{r}'| > d$, where d represents the interdipole distance.

Using Greens' theorem, McConnell and co-workers[15] have shown that eq 3 can be expressed in terms of a double-line integral around the perimeter of the domain:

$$F^{E} = \frac{2\pi}{t} A\mu^2 - \frac{1}{2}\mu^2 I \tag{4}$$

$$I = \oint_C \oint_C \frac{d\mathbf{X}\, d\mathbf{X}'}{|\mathbf{X} - \mathbf{X}'|} \tag{5}$$

Here, t is the thickness of a dipole and $\mathbf{X}$ is the position vector to a point on the perimeter. The line integrals above are constrained such that $|\mathbf{X} - \mathbf{X}'| > d$.

Using polar coordinates, we express the vector $\mathbf{X}$ in the following general form:

$$\mathbf{X} \equiv \mathbf{R}(\theta)\hat{e}_r \tag{6}$$

where $\hat{e}_r$ represents the unit radical vector. The following general relations can then be derived. The perimeter is given by

$$P = \int_0^{2\pi} \left| \frac{d\mathbf{X}}{d\theta} \right| d\theta = \int_0^{2\pi} [R^2(\theta) + R'^2(\theta)]^{1/2}\, d\theta \tag{7}$$

where $R'(\theta) \equiv dR(\theta)/d\theta$. From eq 5, the integral I is given by

$$I = \int\int_{|\theta-\theta'|>\delta} \frac{1}{|\mathbf{X} - \mathbf{X}'|} \frac{d\mathbf{X}}{d\theta} \frac{d\mathbf{x}'}{d\theta'}\, d\theta\, d\theta' \tag{8}$$

$$= \int\int_{|\theta-\theta'|>\delta} (\cos(\theta - \theta')[R(\theta)\, R(\theta') + R'(\theta)\, R'(\theta')] + \sin(\theta - \theta')[R'(\theta)\, R(\theta') - R(\theta)\, R'(\theta')])([R^2(\theta) + R^2(\theta') - 2R(\theta)\, R(\theta') \cos(\theta - \theta')])^{-1/2}\, d\theta\, d\theta' \tag{9}$$

$$\delta(\theta) = d\left| \frac{d\mathbf{X}}{d\theta} \right|^{-1} = \frac{d}{[R^2(\theta) + R'^2(\theta)]^{1/2}} \tag{10}$$

Thus, P and I are readily found by quadrature. In the calculations reported herein, we employed Gaussian quadrature using 600 points for integrals over each variable; the numerical accuracy by this method is better than 0.01%.

We now consider the special case of regularly undulating domains, such as those shown in Figure 2. Such domain shapes are characterized by the following:

$$R(\theta) = \Lambda(1 + \epsilon \cos(m\theta)) \tag{11}$$

where m denotes the mode, Λ the mean radius, and ϵ the relative amplitude of the undulation. The relative amplitude ranges from zero to one: at $\epsilon = 0$ the shape is circular; at $\epsilon = 1$ the shape of the domain pinches off at the origin, i.e., the domain falls apart into m pieces.

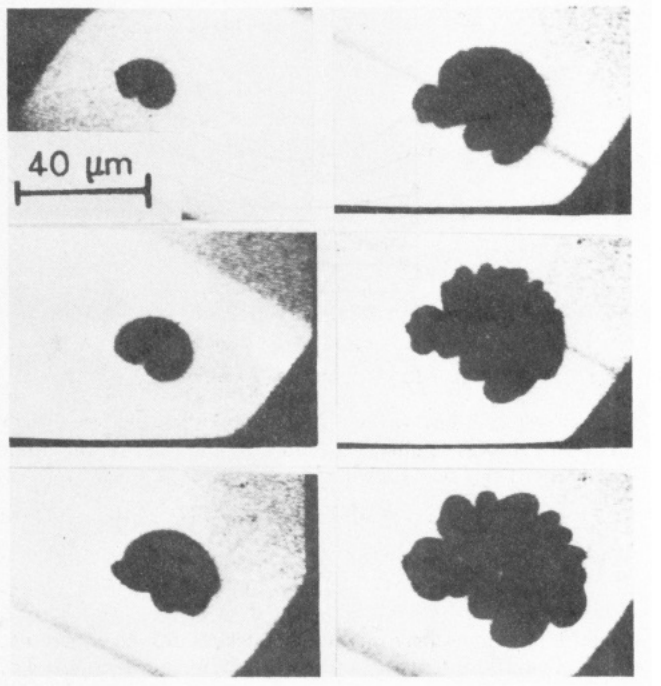

Figure 1. Growth of an isolated DPPC domain fixed under an electrode mounted above the water surface, taken from the work of Flörsheimer.[17] The shape of the domain is stable over a period of hours.

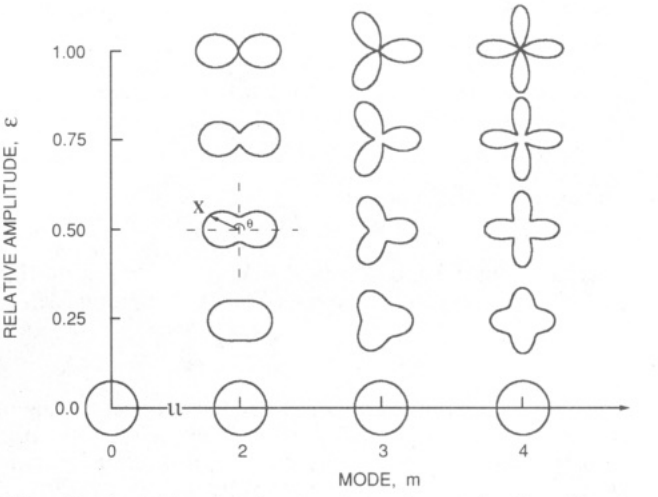

Figure 2. Regularly undulating domains as characterized by a discrete mode, m, and relative amplitude of the undulation, ϵ.

We consider those shapes with $m \geq 2$ and with $m = 0$, the latter corresponding to a circular shape. The shape corresponding to $m = 1$ represents only a translation of the circular domain at small ϵ, cannot be qualitatively described as a domain with a regularly undulating boundary, and hence will not be considered.

For $m > 0$, the area of the domain is independent of the mode and is given by

$$A = \pi\Lambda^2(1 + 0.5\epsilon^2) \tag{12}$$

In the free energy calculations which follow, the area of the domain is fixed. Hence, we take ϵ to be the independent variable, with Λ determined by eq 12. The radius of the circular ($m = 0$) domain with equivalent area is thus given by

$$R_0 = \Lambda[(1 + 0.5\epsilon^2)]^{1/2} \tag{13}$$

For a circular domain shape with radius R_0, the following results are easily derived:

$$P_0 = 2\pi R_0 \tag{14}$$

$$I_0 = 4\pi R_0 \ln(4R_0/e^2 d) \tag{15}$$

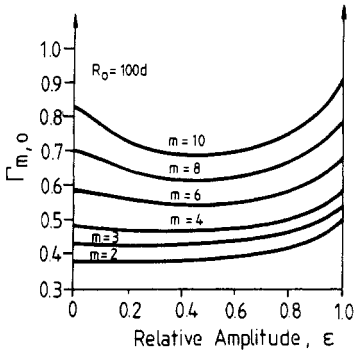

Figure 3. Variaton of $\Gamma_{m,0}$ with relative amplitude, ϵ.

From eq 1, 2, and 4, the difference between the free energy of an undulating domain, with mode m and relative amplitude ϵ, and a circular domain with the same area is given by

$$\Delta F(m,\epsilon;A) = \lambda[(P - P_0) + \tfrac{1}{2}\Gamma(I - I_0)] \quad (16)$$

where

$$\Gamma \equiv \mu^2/\lambda \quad (17)$$

Here, Γ is a dimensionless number which relates the importance of electrostatic interactions to the effect of line tension. The competition between these two interactions, as defined by Γ, determines the equilibrium domain shape. In all that follows, we report the free energy of every domain relative to that of a circular domain with equivalent area, as defined by eq 16, in a dimensionless form obtained by dividing by $R_0\lambda$, where R_0 is the radius of the circular domain.

In addition to regularly undulating domains, as defined by eq 11, we also consider "mixed mode" domains whose shapes can be described as a linear combination of two modes. In this case

$$R(\theta) = \Lambda_m(1 + \epsilon_m \cos(m\theta)) + \Lambda_n(1 + \epsilon_n \cos(n\theta)) \quad (18)$$

The area of a such a domain is

$$A = A_m + A_n + 2\pi\Lambda_m\Lambda_n \quad (19)$$

where A_m is given by eq 12 with $\Lambda = \Lambda_m$ and $\epsilon = \epsilon_m$. We define χ_m to be the area fraction corresponding to the mth mode:

$$\chi_m \equiv \frac{A_m + \pi\Lambda_m\Lambda_n}{A} \quad (20)$$

Thus, χ_m ranges from zero to one, the limits corresponding to regularly undulating domains with modes m and n, respectively. At fixed domain area, we take χ_m, ϵ_m, and ϵ_n to be the independent variables, with Λ_m and Λ_n determined from eq 19 and 20.

Results

We examine first the variation of the free energy of an mth mode regularly undulating domain with the relative amplitude of the undulation, ϵ, and consequently predict the shape transition between a circular domain and the mth mode regularly undulating domain. Results are calculated for a fixed domain area, equal to that of a circular domain with $R_0 = 100d$. We define $\Gamma_{m,0}$ to be the value of Γ such that the free energy of the mth mode domain is equal to that of a circular domain with equivalent area, i.e., $\Delta F(m,\epsilon;A) = 0$. Note from eq 16 that since $P - P_0 \geq 0$ and $I - I_0 \leq 0$, then for $\Gamma > \Gamma_{m,0}$ the undulating domain is more stable than the circular domain, i.e., $\Delta F(m,\epsilon;A) < 0$. Conversely, for $\Gamma < \Gamma_{m,0}$, the circular domain is more stable.

Figure 3 shows the variation of $\Gamma_{m,0}$ with relative amplitude for modes ranging from 2 to 10. For each mode, a shape transition between the corresponding undulating domain and a circular domain exists and occurs at Γ equal to the minimum value of $\Gamma_{m,0}$ denoted by $\Gamma^*_{m,0}$; the relative amplitude corresponding to $\Gamma^*_{m,0}$ is denoted by $\epsilon^*_{m,0}$. At $\Gamma = \Gamma^*_{m,0}$, the free energy of the mth mode undulating domain with relative amplitude $\epsilon^*_{m,0}$ is equal to that of a circular domain with equivalent area. For $\Gamma > \Gamma^*_{m,0}$, the mth mode domain has, over a range of relative amplitudes about $\epsilon^*_{m,0}$, a lower free energy than the circular domain.

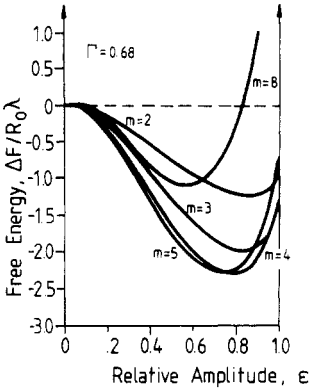

Figure 4. Free energy of undulating domains (relative to that of a circular domain with $R_0 = 100d$) vs the relative amplitude of the undulation, ϵ, for various modes. At this Γ, two distinct modes ($m = 4$ and $m = 5$) have the lowest free energy.

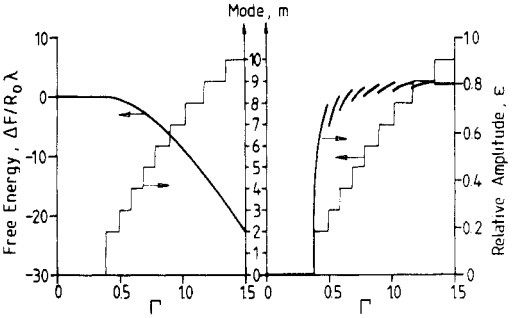

Figure 5. Variation with Γ of the free energy, mode, and relative amplitude of the regularly undulating domains with minimum free energy. The areas of the domains are fixed and equal to that of a circular domain with $R_0 = 100d$.

For all modes greater than two, $\epsilon^*_{m,0} > 0$; thus, the predicted shape transitions between circular domains and these undulating domains are first-order, i.e., discontinuous. However, for the second mode, $\epsilon^*_{2,0} = 0$, at which point the undulating domain has the limiting circular shape. Thus, the shape transition between a circular domain and an undulating domain with $m = 2$ is second-order, in agreement with predictions by McConnell and coworkers[15] for the circular–elliptical shape transition. They showed analytically that this transition occurs at $\Gamma = \ln^{-1}[4R_0/e^{10/3}d]$, in agreement with our numerical results.

We have thus far examined only the possibility of a shape transition between a circular domain and a regularly undulating domain with fixed mode. It is readily noted from Figure 3 that $\Gamma^*_{m,0} > \Gamma^*_{m-1,0}$. This means that shape transitions between circular domains and undulating domains with modes greater than two would not occur if the system were always in equilibrium. Hence, we now examine the equilibrium shape transitions that are predicted as Γ is continuously varied. For a given Γ, we search for the mode and corresponding relative amplitude of the regularly undulating domain with minimum free energy. Figure 4 shows, for example, the variation with relative amplitude of the free energy, relative to that of a circular domain, for several different modes at $\Gamma = 0.68$. Note that, in this particular case, two different domain shapes have the lowest free energy and can therefore coexist at equilibrium: one with $m = 4$ and $\epsilon = 0.78$ and one with $m = 5$ and $\epsilon = 0.73$.

Figure 5 shows the variation with Γ of the modes and corresponding relative amplitudes of the domain shapes with the lowest free energy. Note that as Γ is increased, higher order modes become more stable. First-order shape transitions are predicted between successive modes, except for the second-order circular to $m = 2$ transition as previously described. Although it is not readily apparent from Figure 5, the slope of the free energy curve is discontinuous at the shape transition points between successive modes. Values of Γ at the predicted shape transitions are given in Table I.

TABLE I: Values of Γ at Shape Transitions between Modes

	$R_0 = 100d$	$R_0 = 300d$	$R_0 = 500d$
$\Gamma_{0,2}$	0.376	0.266	0.234
$\Gamma_{2,3}$	0.491	0.319	0.274
$\Gamma_{3,4}$	0.585	0.356	0.301
$\Gamma_{4,5}$	0.680	0.390	0.325
$\Gamma_{5,6}$	0.783	0.421	0.347
$\Gamma_{6,7}$	0.898	0.452	0.367
$\Gamma_{7,8}$	1.022	0.483	0.388
$\Gamma_{8,9}$	1.173	0.514	0.407
$\Gamma_{9,10}$	1.346	0.544	0.426

TABLE II: Relative Amplitudes at Shape Transitions between Modes

$m, m+1$	ϵ^*_m	ϵ^*_{m+1}
2, 3	0.71	0.63
3, 4	0.75	0.70
4, 5	0.78	0.73
5, 6	0.79	0.76
6, 7	0.80	0.77
7, 8	0.81	0.78
8, 9	0.81	0.79
9, 10	0.82	0.80

As is readily seen from Figure 5, over the range of Γ where a given mode is the most stable, the relative amplitude increases with increasing Γ; hence, the shapes become more elongated. This is consistent with the increasing importance of electrostatic interactions relative to the effect of line tension. On the other hand, Figure 5 also reveals that as Γ is increased, the relative amplitude of the most stable mode asymptotes to a limit, ca. 0.81. This implies that a regularly undulating domain with relative amplitude equal to one is never the most stable state, and hence, within the class of shapes considered, an energy barrier must be overcome for domain fission.

Next, we examine the effect of area on the predicted shape transitions. Included in Table I are values of Γ at the equilibrium shape transitions for domains with area equal to that of a circle with $R_0 = 300d$ and $R_0 = 500d$. The effect of increasing area is thus to shift the occurrence of all shape transitions to lower Γ and to simultaneously decrease the range of Γ over which a given mode is the most stable. It is important to note that while the occurrence of each shape transition depends on Γ, the relative amplitudes at the transition points, denoted by ϵ^*_m and ϵ^*_{m+1}, are independent of area. These are listed in Table II.

We have so far considered only regularly undulating domains, each characterized by a single "pure" mode. We now examine the possibility of mode coupling, i.e., domains whose shape can be described as a combination of two modes, as defined by eq 18.

First, we examine mode coupling at the shape transition points between successive modes. At each transition point, we calculate the free energy of the mixed-mode domains formed by combining the two corresponding pure-mode domain shapes which can coexist in equilibrium. Thus, for a given domain area, we set the relative amplitudes equal to ϵ^*_m and ϵ^*_{m+1}, as given in Table II, and vary the area fraction of the mth mode, χ_m. The variation with area fraction of the free energy of such mixed-mode domains is shown in Figure 6. In all cases examined, the limiting pure-mode domain shapes have the lowest free energy, and hence there is no mode coupling. In addition, as higher order modes are combined, the free energy of the mixed-mode shape becomes increasingly greater than the free energy of the limiting pure-mode shapes.

The mixed-mode analysis can be extended in the following way: at fixed area, the free energy of a mixed-mode domain is minimized with respect to both the area fraction *and* relative amplitudes of the two modes. We examined two different mixed-mode combinations: shapes formed by combining the third and fourth modes, and shapes formed by combining the second and fourth modes. In both cases, the domain area was set equal to that of a circular domain with $R_0 = 100d$.

Figure 7 shows the variation with Γ of the free energy of the most stable domains formed by mixing the third and fourth modes. This is compared to the free energy of the most stable pure-mode

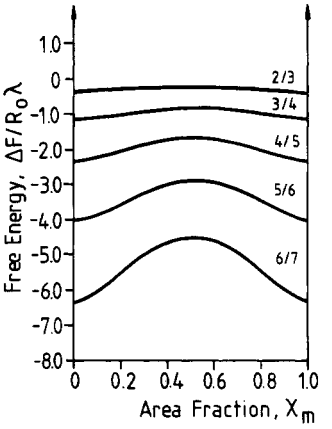

Figure 6. Variation with area fraction of the free energy (relative to that of a circular domain with $R_0 = 100d$) of mixed-mode domains formed by combining successive pure-mode shapes which can coexist in equilibrium.

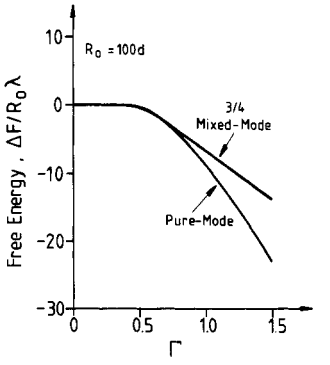

Figure 7. Variation with Γ of the free energy (relative to that of a circular domain with $R_0 = 100d$) of the most stable mixed-mode domains formed by combining the third and fourth modes.

shapes. Over the entire range of Γ, the 3/4 mixed-mode domains have free energy equal to or higher than the free energy of the most stable pure-mode domains, the former case occurring only when the mixed-mode shape has a limiting pure-mode form, i.e., when $\chi_3 = 0$ or 1. It is also of interest to note that, in all cases, the 3/4 mixed-mode domains of lowest free energy have one of the two relative amplitudes equal to zero (cf. eq 18). This corresponds to combining a regularly undulating domain with a circular domain; hence, the boundaries of the 3/4 mixed-mode shapes with minimum free energy are themselves regularly undulating.

Like the previous case, mixed-mode shapes formed by combining the second and fourth modes have free energy higher than or equal to the free energy of the most stable pure-mode shapes, with one exception: over a small range of Γ (beginning at $\Gamma_{0,2}$), the most stable 2/4 mixed-mode shapes have slightly lower free energies than the most stable pure-mode shapes. Recall that $\Gamma_{0,2}$ corresponds to the point at which a circular domain undergoes a second-order shape transition into an $m = 2$ regularly undulating domain. As McConnell and co-workers have shown,[15] this shape transition point corresponds to one at which a circular shape crosses over to any noncircular shape. It is thus not surprising that different shapes can have nearly the same free energy. For example, from $0.376 < \Gamma < 0.413$, 2/4 mixed-mode domains which are nearly elliptical (with $\epsilon_2 = 0.50$, $\epsilon_4 = 0.20$, and $\chi_2 = 0.75$) have minimum free energy. For $\Gamma > 0.413$, however, the most stable pure-mode shapes have free energies lower than or equal to that of the most stable 2/4 mixed-mode shapes.

Discussion and Conclusions

We have investigated the possible shape transitions of domain shapes with regularly undulating boundaries. The equilibrium shapes and corresponding shape transitions are governed by a dimensionless number, Γ, which relates the importance of elec-

trostatic interactions to the effect of line tension. Experimentally, however, Γ is nearly constant for a given lipid system at fixed temperature.

By use of fluorescence film balance techniques,[5-7] the microstructure of the two-dimensional lipid system is typically observed along a pressure–area isotherm. In the fluid/gel coexistence region, the fraction of molecules in the gel phase increases as the total average area per molecule is decreased. As this happens, the gellike domains generally increase in size, rather than in number.[10] The theoretical analysis presented in this work can be applied to the behavior of equilibrium shapes observed experimentally as the area of the domains is varied.

Recall that as the domain area is increased, the value of Γ at each predicted equilibrium shape transition decreases continuously. This implies that, at fixed Γ, shape transitions occur as the area is varied, with higher order modes becoming more stable with increasing area. In other words, the variation with domain area of the mode and relative amplitude of the shape with lowest free energy is qualitatively similar to the variation with Γ, as shown in Figure 4. For example, at some critical domain area, a regular undulating domain with mode m and relative amplitude ϵ^*_m can coexist with a domain with mode $m + 1$ and relative amplitude ϵ^*_{m+1}. Over the range of areas where a given mode is the most stable, the relative amplitude increases with increasing area.

Note that circular domains become the most stable as the area is decreased. This is in agreement with experimental observations of small domains observed just after nucleation;[10] these are generally circular. Based on the analysis above, the following shape transitions are then predicted: as the domains are further grown, the circular domains will become unstable and undergo a continuous second-order transition to an $m = 2$ mode domain. At progressively larger areas, the domain undergoes a series of first-order shape transitions between successive modes. The area corresponding to a given shape transition between two successive modes is, of course, a function of Γ. The larger the Γ, the smaller the area at each predicted shape transition.

While higher order modes become continuously favored as the area is increased, the relative amplitude of the equilibrium domain shape asymptotes to a constant value. Thus as their sizes increase, the domains sprout additional protrusions while their shapes remain qualitatively similar. Furthermore, a domain shape that is pinched off at the center never has the lowest free energy.

We also investigated the possibility of mode coupling. In all cases examined, the free energy of mixed-mode domains formed by combining two successive modes was equal to or higher than that for regularly undulating (pure-mode) shapes. The analysis also revealed that the lowest free energy of mixed-mode shapes is in general obtained for a combination of shapes where one amplitude equals zero.

We note that we have examined only one, albeit large, class of domain shapes: those that can be described as regularly undulating (and those formed by a linear combination of two such shapes). Hence, we cannot account for, nor predict, domain shapes and associated shape transitions that do not fall within this classification. On the other hand, many lipid systems form domains with shapes that are qualitatively similar to those considered.

We also note that the calculations presented herein are strictly valid for systems in equilibrium and in the low-temperature limit.[14] Experimentally, the attainment of thermodynamic equilibrium is quite questionable; in fact, it has been demonstrated[10] that the nucleation and growth of domains depend on the compression speed, temperature, and impurity content. Yet, with respect to their shape, it appears domains can reach a metastable state,[15] and within this context the analsyis presented herein may be applied.

Finally, recall that the shapes and associated shape transitions of the dipolar lipid domains, as predicted by the free energy theory, are governed by a dimensionless number, Γ, as defined in eq 17. Γ accounts for the competition between the long-range repulsive electrostatic interactions and the effect of line tension. Unlike line tension, the excess dipole moment normal to the interface is experimentally accessible from surface potential measurements. Thus, the analysis presented here offers a means to indirectly measure the line tension from quantitative measurements of the various shapes and corresponding shape transitions that are predicted. This is currently one focus of experimental work in our laboratory and will be the subject in a forthcoming publication.

Acknowledgment. The authors gratefully acknowledge a NATO Postdoctoral Fellowship awarded to T.K.V. and the Deutsche Forschungsgemeinschaft for financial support of this research.

Catalytic Oxidation and Isotopic Exchange of Hydrogen over 12-Molybdophosphoric Acid†

Noritaka Mizuno,* Tetsuji Watanabe,‡ and Makoto Misono*

Department of Synthetic Chemistry, Faculty of Engineering, The University of Tokyo, Hongo, Bunkyo-ku, Tokyo 113, Japan *(Received: June 22, 1989)*

The reactions of H_2, such as H_2–D_2 isotopic equilibration and exchange, reduction of catalyst by H_2 (noncatalytic oxidation of H_2 by a catalyst), and catalytic oxidation of H_2, have been studied mostly at 573 K over 12-molybdophosphoric acid (PMo_{12}) and its Na salt. The isotopic equilibration and exchange were apparently very slow, although the uptake of H_2 proceeded at a considerable rate. This was in marked contrast to 12-tungstophosphoric acid (PW_{12}) studied previously, for which the equilibration and exchange were very rapid, while the H_2 uptake was negligible. The present results were explained by numerical simulation, which revealed that the accumulation of protons and subsequent formation of water from proton and polyanion took place nearly uniformly in the bulk of PMo_{12} at a rate comparable with the H_2 uptake. Due to this, the rates of reduction and the catalytic oxidation of H_2 were almost independent of their specific surface area (thus called "bulk-type catalysis, type II").

Introduction

Heteropoly compounds are useful catalysts in both acid and oxidation catalysis. In particular, 12-heteropoly compounds are practically used in several industrial processes.[1]

In oxidation catalysis, the dynamics of the reduction–oxidation of catalysts is important. We have previously reported that heteropoly compounds have interesting reduction–oxidation

† Part 15: Catalysis by Heteropoly Compounds.

‡ Present address: Central Research Laboratory, Nippon Oil Co., Ltd., Yokohama 231, Japan.

(1) Misono, M. *Catal. Rev.* **1987**, *29*, 269–321, and references cited therein.

0022-3654/90/2094-0890$02.50/0